Atmos. Meas. Tech., 5, 1601–1609, 2012
www.atmos-meas-tech.net/5/1601/2012/
doi:10.5194/amt-5-1601-2012

Atmospheric Measurement Techniques

Site selective real-time measurements of atmospheric N_2O isotopomers by laser spectroscopy

J. Mohn[1], B. Tuzson[1], A. Manninen[1], N. Yoshida[2], S. Toyoda[2], W. A. Brand[3], and L. Emmenegger[1]

[1]Laboratory for Air Pollution & Environmental Technology, Empa, Dübendorf, Switzerland
[2]Department of Environmental Chemistry and Engineering, Tokyo Institute of Technology, Yokohama, Japan
[3]Max-Planck-Institute for Biogeochemistry, Jena, Germany

Correspondence to: J. Mohn (joachim.mohn@empa.ch)

Received: 3 January 2012 – Published in Atmos. Meas. Tech. Discuss.: 23 January 2012
Revised: 29 May 2012 – Accepted: 11 June 2012 – Published: 11 July 2012

Abstract. We describe the first high precision real-time analysis of the N_2O site-specific isotopic composition at ambient mixing ratios. Our technique is based on mid-infrared quantum cascade laser absorption spectroscopy (QCLAS) combined with an automated preconcentration unit. The QCLAS allows for simultaneous and specific analysis of the three main stable N_2O isotopic species, $^{14}N^{15}N^{16}O$, $^{15}N^{14}N^{16}O$, $^{14}N^{14}N^{16}O$, and the respective site-specific relative isotope ratio differences $\delta^{15}N^{\alpha}$ and $\delta^{15}N^{\beta}$. Continuous, stand-alone operation is achieved by using liquid nitrogen free N_2O preconcentration, a quasi-room-temperature quantum cascade laser (QCL), quantitative sample transfer to the QCLAS and an optimized calibration algorithm. The N_2O site-specific isotopic composition ($\delta^{15}N^{\alpha}$ and $\delta^{15}N^{\beta}$) can be analysed with a long-term precision of 0.2 ‰. The potential of this analytical tool is illustrated by continuous N_2O isotopomer measurements above a grassland plot over a three week period, which allowed identification of microbial source and sink processes.

1 Introduction

Nitrous oxide (N_2O) is the most important anthropogenic emitted ozone depleting substance and also a significant greenhouse gas (Ravishankara et al., 2009). N_2O mixing ratios in the troposphere increased from 270 ppb to the current level of 321.6 ppb at 0.8 ppb yr^{-1} (2005 to 2008) with more than one third of N_2O emissions being anthropogenic (Montzka et al., 2011; Solomon et al., 2007). For a better understanding of source and sink processes, however, the information obtained from measuring the intramolecular distribution of ^{15}N on the central (α) and the end (β) position of the linear N_2O molecule is crucial (Yoshida and Toyoda, 2000).

Abundances of the different isotopic species ($^{14}N^{14}N^{16}O$, $^{14}N^{15}N^{16}O$, $^{15}N^{14}N^{16}O$, etc.) are usually reported in the δ-notation, where $\delta^{15}N$ denotes the relative difference in the amount of ^{15}N versus ^{14}N (abbreviated herein as $^{15}N/^{14}N$) in N_2O in comparison to atmospheric N_2 as the reference material (Coplen, 2011). Similarly, $\delta^{15}N^{\beta}$ denotes the relative difference of isotope ratios for $^{15}N^{14}N^{16}O$ versus $^{14}N^{14}N^{16}O$.

The bulk nitrogen δ value ($\delta^{15}N^{bulk} = (\delta^{15}N^{\alpha} + \delta^{15}N^{\beta})/2$) of tropospheric N_2O is enriched by 6.3 ± 0.3 ‰ to 6.72 ± 0.12 ‰, depending on the sampling location and time (Kaiser et al., 2003; Park et al., 2004; Röckmann and Levin, 2005; Toyoda et al., 2004), with a strong site preference ($SP = \delta^{15}N^{\alpha} - \delta^{15}N^{\beta}$) of 18.7 ± 2.2 ‰ for the central nitrogen atom (Yoshida and Toyoda, 2000). Temporal trends in the N_2O isotopic composition from firn air, ice core and archived air sample measurements indicate a year to year decrease in $\delta^{15}N^{bulk}$ of 0.04 ‰ yr^{-1}, confirming substantial emissions of isotopically depleted N_2O (Bernard et al., 2006; Ishijima et al., 2007; Röckmann and Levin, 2005). According to isotopic budgetary calculations based on a simple two-box model, this could be due to increased anthropogenic N_2O emission from agricultural soils, as well as a to a change in their average isotopic signature (Ishijima et al., 2007).

On a local scale, the N_2O isotopic composition can be applied to disentangle or even quantitatively apportion N_2O production and destruction pathways. For example, the ^{15}N depletion in N_2O produced by autotrophic nitrification was

found to be considerably higher as compared to heterotrophic denitrification (Koba et al., 2009; Sutka et al., 2006; Toyoda et al., 2005; Yoshida, 1988). On the other hand, process-specific effects on $\delta^{15}N^{bulk}$ might be masked by shifts in the precursor signature (Well et al., 2008), and theoretical considerations indicate a major impact of the involved bacterial species (Schmidt et al., 2004). In contrast to $\delta^{15}N^{bulk}$, the site preference is considered to be independent of the isotopic composition of the precursor and, thus, supplies clear process information even if the isotopic signature of the substrate for N_2O production is lacking (Frame and Casciotti, 2010; Ostrom et al., 2007; Sutka et al., 2006; Toyoda et al., 2002; Yamagishi et al., 2007; Well and Flessa, 2009).

The standard technique for N_2O isotopic measurements is laboratory-based isotope-ratio mass-spectrometry (IRMS) in combination with flask-sampling (Brenninkmeijer and Röckmann, 1999; Toyoda and Yoshida, 1999). It is a well-known method with excellent precision of up to 0.05 ‰ for $\delta^{15}N^{bulk}$, 0.1 ‰ for $\delta^{18}O$, and 0.3 ‰ for $\delta^{15}N^{\alpha}$ and $\delta^{15}N^{\beta}$ (Bernard et al., 2006; Toyoda et al., 2011a, b). Nevertheless, it also has some disadvantages such as the large size of the instrument, which hinders in situ field measurements. Laser spectroscopy is a valuable alternative because it is inherently selective, even for molecules with the same mass (Janssen and Tuzson, 2006; Gagliardi et al., 2005; Nakayama et al., 2007; Uehara et al., 2001, 2003; Wächter and Sigrist, 2007), and field-deployable instruments for unattended measurements can be designed. A significant improvement was obtained in recent years by the implementation of quantum cascade laser absorption spectroscopy (QCLAS) to reach a precision of 0.5 ‰ for $\delta^{15}N^{\alpha}$ and $\delta^{15}N^{\beta}$ at N_2O mixing ratios of 90 ppm (Wächter et al., 2008). Other important techniques for isotope ratio measurements include cavity ring-down spectroscopy (CRDS) (Crosson, 2008) and off-axis integrated cavity output spectroscopy (OA-ICOS) (Baer et al., 2002). These methods have been widely used in the near infrared spectral region. Recently, commercial CRDS and OA-ICOS instruments with mid-IR QC lasers have been announced, taking advantage of the fact that the absorption of N_2O is more than 4 orders of magnitude stronger in the MIR as compared to the NIR.

In the present project, we describe the first instrumentation to perform real-time analysis of N_2O site-specific isotopic composition at atmospheric mixing ratios. This is achieved combining a liquid nitrogen-free fully-automated preconcentration unit optimized and validated for N_2O isotopomer analysis by Mohn et al. (2010) with an improved version of the QCLAS published by Wächter et al. (2008). The potential of this approach is demonstrated by a three week measurement campaign of atmospheric N_2O to identify distinct soil microbial N_2O source and sink processes.

2 Materials and methods

A schematic diagram of the measurement setup is shown in Fig. 1. Details on the development, optimization and validation of the N_2O preconcentration unit and the QC laser spectrometer have been described previously (Mohn et al., 2010; Wächter et al., 2008). Thus, their basic principles and recent modifications are only briefly presented, while analytical improvements, procedures of air sampling, automation and the applied calibration procedure are discussed in more detail.

2.1 Sampling site and setup

Field experiments were conducted in Dübendorf at 430 m a.s.l. (47°24′10″ N/8°36′43″ E). The observation area is located in an industrial and densely populated region near Zurich. A main road passes 100 m south and a highway around 750 m north of the sampling site. Measurements were executed from 8 to 31 September 2010 on a grassland plot (5 m × 20 m) which was fertilized on 22 September (220 kg N ha^{-1} NH_4NO_3, 400 kg C ha^{-1} sucrose). Air was continuously sampled at a flow rate of about one standard litre per minute (slpm) through a 15 m long unheated PTFE tubing (ID 4 mm) using a diaphragm vacuum pump (KNF Neuberger, Switzerland). The air intake was first mounted at 1.5 m above ground (8 to 24 September), and then (24 to 31 September) 10 cm above the surface to be more representative for soil N_2O production. At the pump outlet, the pressure was adjusted to 4 bar by means of a pressure relief valve. Water and CO_2 were quantitatively removed by permeation drying (PD-100T-48, PermaPure Inc., USA) and by chemical trapping with Ascarite (30 g, 10–35 mesh, Fluka, Switzerland) bracketed by $Mg(ClO_4)_2$ (2 × 13 g, Fluka, Switzerland). Finally, the sample was passed through a sintered metal filter (SS-6F-MM-2, Swagelok, USA) and directed to the preconcentration unit. An alternative sample input consisted of pressurized air (Messer, Switzerland) employed as target gas which was treated as described above by a second permeation dryer and a chemical trap (20 g Ascarite, 2 × 8 g $Mg(ClO_4)_2$). This setup allows determining the long-term stability and precision of the complete analytical procedure, including preconcentration, laser spectroscopic analysis and calibration. The chemical traps were exchanged every 3 to 4 days before reaching their maximal load. To detect any potential breakthrough, the CO_2 concentration was monitored by QCLAS after preconcentration together with the N_2O isotopomers (CO_2 line at 2188.0 cm^{-1}).

2.2 Instrumentation

2.2.1 N_2O preconcentration

The technology of our preconcentration unit is based on a previously developed system called “Medusa” (Miller et al., 2008), re-designed and optimized for the preconcentration of N_2O isotopic species and their subsequent quantification by

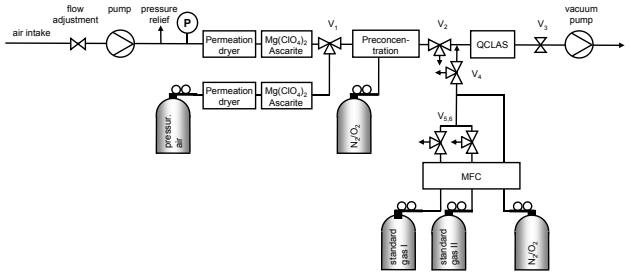

Fig. 1. Experimental setup for online N_2O isotopomer analysis in ambient air. Vi are solenoid valves and MFC mass flow controllers.

laser spectroscopy (Mohn et al., 2010). During standard operation, 10 l of ambient air are preconcentrated on a porous polymer adsorption trap (HayeSep D 100–120 mesh, Hayes Separations Inc., USA) at a flow rate of 500 sccm (standard cubic centimetre per minute) within 20 min. Desorption is accomplished by 10 sccm of synthetic air, within approximately 5 min, yielding a concentration increase from ambient mixing ratios to >71 ppm N_2O. The system offers quantitative (>99 %) N_2O recovery without any significant isotopic fractionation or relevant spectral interferences from other atmospheric constituents. Modifications to the previous procedure (Mohn et al., 2010) are mainly related to the desorption phase, where the N_2O concentration profile was further optimized by increasing the trap temperature to 10 °C and decreasing the flow rate of high purity synthetic air to 10 sccm.

2.2.2 Laser spectrometer

The employed QCLAS is based on the instrument described by Wächter et al. (2008). It consists of a single-mode, pulsed QCL emitting at 2188 cm^{-1}, a multipass absorption cell (optical path length 56 m, volume 0.5 l; Aerodyne Research Inc., USA) and a detection system with pulse normalization. Laser control, data acquisition and simultaneous quantification of the three main N_2O isotopic species ($^{14}N^{14}N^{16}O$, $^{15}N^{14}N^{16}O$, $^{14}N^{15}N^{16}O$) is accomplished by the TDLWintel software (Aerodyne Research Inc., USA), taking into account path length, gas temperature ($\sim$ 305 K), pressure (8 kPa) and laser line width (0.0068 cm^{-1}). Gas temperature was stabilized to 0.05 K and additionally monitored by a calibrated 10 kΩ thermistor (TCS-610, Wavelength Electronics Inc., USA). Employing a new generation thermo-electrically cooled detector (PVI-3TE-5, Vigo System, PL), a new quasi-room temperature QCL (Alpes Lasers SA, Switzerland) and redesigned electronics led to a considerably improved performance of the laser spectrometer, compared to the results of Wächter et al. (2008).

Applying the Allan variance approach (Werle, 2011) for the site-specific relative difference of isotope ratios $\delta^{15}N^{\alpha}$ and $\delta^{15}N^{\beta}$, a short-term precision of 1 ‰ $Hz^{-1/2}$ is achieved at mixing ratios of 70 ppm N_2O, as typically obtained by preconcentration of atmospheric N_2O. For six minutes spectral averaging a precision below 0.1 ‰ is obtained, which is almost one order of magnitude lower than previously published (Wächter et al., 2008). The maximum precision at 30 min averaging corresponds to 0.04 ‰, for both $\delta^{15}N^{\alpha}$ and $\delta^{15}N^{\beta}$. The minimum equivalent absorbance of 4.1×10^{-6} was calculated based on the absorption spectrum and Allan variance plot.

The laser spectrometer was operated in a batch mode, where the gas cell was first evacuated by a scroll pump (TriScroll 300, Varian, USA), then purged for 4 min with 10 sccm of purge gas at reduced pressure (1 kPa), before the downstream on-off valve (V3 in Fig. 1) (2-way, 009-0089-900, Parker Hannifin Corp., USA) was closed. The purge gas was either synthetic air (prior to analysis of preconcentrated ambient or pressurized air) or calibration gas (prior to calibration). Subsequently, the multipass cell was filled with preconcentrated air or calibration gas to a cell pressure of 8 kPa (±0.02 kPa) monitored by means of a capacitance manometer (722A, MKS Instruments, USA). Finally, the multipass cell was closed by switching the 3-way valve V2 or V4 (009-0933-900, Parker Hannifin Corp., USA) before the gas sample was analysed.

2.3 Automation and measurement procedure

The complete experimental setup including preconcentration unit, solenoid valves (V1–V6, Parker Hannifin Corp., USA) and thermal mass flow controllers (MFCs, Redy Smart series, Vögtlin Instruments, Switzerland) was controlled and monitored by a LabVIEW programme (National Instruments Corp., USA). All peripherals were connected through a 16-port serial to Ethernet connector (EL-160, Digi International Inc., USA). For ambient air monitoring, a 460 min measuring cycle was repeated which consists of the following steps (Fig. 2): (A) analysis of preconcentrated N_2O from compressed air (target gas, one sample) and ambient air (three gas samples), (B) analysis of standard II (two replicates) dynamically diluted to 71 ppm N_2O with synthetic air to calibrate the δ scale, (C) identical to (A), (D) analysis of standard I (88 ppm N_2O, two replicates) to calibrate N_2O mixing ratios and determine their influence on δ values. Between gas samples (A)–(D), standard I (71 ppm N_2O) was analysed as a reference point and to correct for drift effects.

2.4 Analysis of N_2O mixing ratios and isotopomer ratios

The N_2O mixing ratios of ambient air were determined based on the concentration of the main isotopic species $^{14}N^{14}N^{16}O$ and calibrated against laboratory standard I dynamically diluted to different concentration levels (see Fig. 2 step D). The preconcentration step was taken into account via the ratio of the gas volume in the multipass cell (V_{cell}) and the gas volume applied for N_2O preconcentration (V_{precon}). While V_{precon} can be accurately computed based on the adsorption time and flow, for V_{cell} this is not possible. Therefore, the

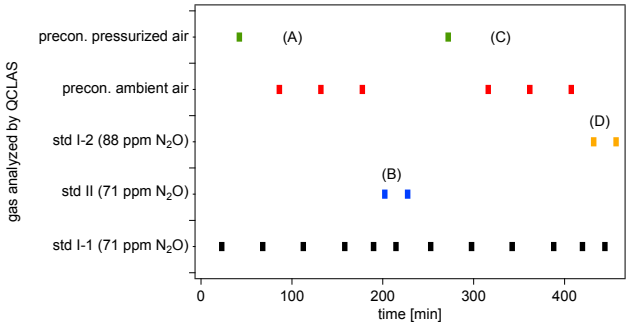

Fig. 2. Measurement cycle: (A) + (C) analysis of ambient air or pressurized air (target gas), (B) determination of calibration factors for $\delta^{15}N^{\alpha}$, $\delta^{15}N^{\beta}$, and (D) the N_2O mixing ratio as well as its influence on δ values.

exact value for V_{cell} under standard conditions was determined analysing preconcentrated N_2O from a highly accurate standard (319.91 ± 0.12 ppb) provided by the World Meteorological Organization (WMO) Central Calibration Laboratory (CCL) (Hall et al., 2007). N_2O concentrations of the laboratory standards were quantified by QCLAS against commercial calibration gases (90.5 ± 0.1 ppm N_2O, Messer, Switzerland) and are indicated in Table 1.

Relative differences of isotopic ratios $\delta^{15}N^{\alpha}$ and $\delta^{15}N^{\beta}$ were determined employing a set of standard gases produced in our laboratory based on gravimetric and dynamic dilution methods from pure medical N_2O (Messer, Switzerland) supplemented with distinct amounts of isotopically pure (>98 %) $^{15}N^{14}N^{16}O$ and $^{14}N^{15}N^{16}O$ (Cambridge Isotope Laboratories, USA). Primary laboratory standards were analysed for $\delta^{15}N^{\alpha}$, $\delta^{15}N^{\beta}$ and $\delta^{15}N^{bulk}$ by IRMS at the Tokyo Institute of Technology. The IRMS reference values for $\delta^{15}N^{bulk}$ was determined by mass analysis of molecular ion (N_2O^+) whereas site-specific $\delta^{15}N^{\alpha}$ (central N) was determined by mass analysis of fragment ion (NO^+). The $\delta^{15}N^{\beta}$ was computed from $\delta^{15}N^{bulk}$ and $\delta^{15}N^{\alpha}$. Details are described in Toyoda and Yoshida (1999). Table 1 indicates the isotopic composition of the secondary laboratory standards applied in the current project and analysed against primary standards by QCLAS. The $\delta^{15}N^{bulk}$ of pure medical N_2O was additionally analysed by mass spectrometry at the IsoLab of the Max-Planck Institute for Biogeochemistry (MPI-BGC, Jena, Germany) using an EA/IRMS setup (Werner et al., 1999). N_2O was introduced in between the combustion and the reduction tube of the EA using the loop (250 µl) of a manually operated 6-port valve. This setup enabled a direct comparison of N_2 produced from combustion of IAEA-N1 to N_2 obtained from the medical N_2O by reduction in the 2nd EA reactor. Quantitative N_2O conversion reaction yield was verified by the absence of any m/z 44 ion current response following N_2O introduction. Using a $\delta^{15}N$ value of +0.43 ‰ for IAEA-N1 as the scale anchor, a $\delta^{15}N^{bulk}$ value of 1.64 ± 0.10 ‰ ($n = 4$) was obtained

Table 1. N_2O mixing ratios and relative differences of isotopic ratios $\delta^{15}N^{\alpha}$ and $\delta^{15}N^{\beta}$ of secondary laboratory standards applied in the current project (the precision indicated is the standard error of the mean). Standard Ia was replaced by standard Ib 22 September.

	N_2O [ppm]	$\delta^{15}N^{\alpha}$ [‰]	$\delta^{15}N^{\beta}$ [‰]
Standard Ia	246.9 ± 0.1	2.1 ± 0.1	2.0 ± 0.2
Standard Ib	250.1 ± 0.05	15.2 ± 0.1	2.0 ± 0.1
Standard II	249.1 ± 0.1	25.0 ± 0.1	24.8 ± 0.2

which was different by 0.39 ‰ from the Tokyo Tech result. A similar difference of 0.3 ‰ was observed by Toyoda and Yoshida (1999) for $\delta^{15}N^{bulk}$ of a laboratory standard calculated from $\delta^{15}N^{\alpha}$ and $\delta^{15}N^{\beta}$ (calibration via NH_4NO_3 decomposition) and determined after N_2O to N_2 reduction. Discrepancies were attributed to fractionation during incomplete NH_4NO_3 decomposition (Toyoda and Yoshida, 1999).

Relative differences of site – selective isotope ratios $\delta^{15}N^{\alpha}$ and $\delta^{15}N^{\beta}$ of preconcentrated N_2O were corrected for dependency of the isotope ratios on the N_2O mixing ratio (before preconcentration). These corrections were small, about 0.004 ‰ ppb^{-1} and 0.016 ‰ ppb^{-1} for $\delta^{15}N^{\alpha}$ and $\delta^{15}N^{\beta}$, respectively. Besides, sudden changes in the laser intensity significantly influenced individual measurements, which were discarded. These light intensity changes affected less than 2 % of the data, and the laser driver that was identified as the source of instability was recently replaced by a different unit (PWS4323, Tektronix Inc., USA).

To confirm the accuracy of our measurements, we analysed background air in a cylinder filled in 2006 by the Earth System Research Laboratory (Global Monitoring Division) of the National Oceanic & Atmospheric Administration (NOAA). The trace gas mixing ratios analysed by the WMO CCL are typical for natural air: 384.40 ± 0.02 ppm CO_2, 319.91 ± 0.12 ppb N_2O, 1838.5 ± 0.4 ppb CH_4, 143.9 ± 1.0 ppb CO. The QCLAS analysis of the N_2O site-selective isotopic composition, with $\delta^{15}N^{\alpha} = 15.62 \pm 0.06$ ‰, $\delta^{15}N^{\beta} = -2.84 \pm 0.04$ ‰, $\delta^{15}N^{bulk} = 6.39 \pm 0.03$ ‰ and $SP = 18.45 \pm 0.08$ ‰ (the precision indicated is the standard error of the mean), is in perfect agreement with published data for unpolluted tropospheric N_2O.

3 Results and discussion

3.1 Continuous analysis of N_2O isotopomers in ambient air

To our knowledge, Fig. 3 presents the first example of real-time analysis of N_2O site-selective isotopic composition. Measurements were conducted for three weeks between 8 and 31 September 2010, corresponding to almost 550 air samples (408 samples of ambient air, 136 target gas samples) that were analysed in a stand-alone operation. During the first

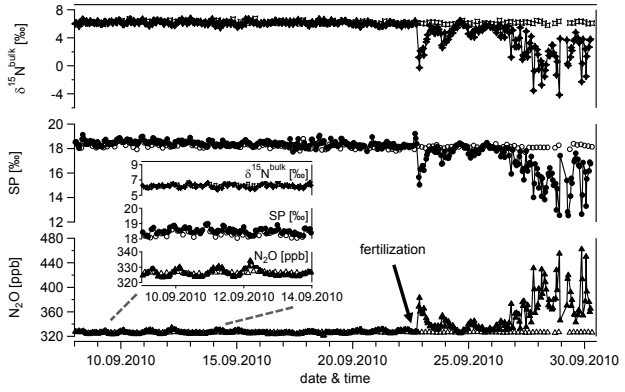

Fig. 3. Time series of N_2O mixing ratio and the corresponding $\delta^{15}N^{bulk}$ and SP values of ambient air (closed symbols) and pressurized air (target gas, open symbols) analysed by QCLAS after preconcentration. Relative isotope ratio differences are based on the Tokyo Tech calibration of the primary laboratory standards. Strong emissions of ^{15}N depleted N_2O were observed after fertiliser addition (200 kg-N ha^{-1} NH_4NO_3, 400 kg-C ha^{-1} sucrose) indicated by an arrow.

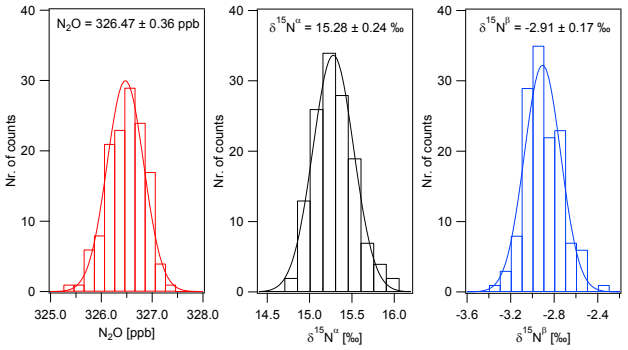

Fig. 4. Repeated measurements of pressurized air (target gas) during the field experiment. N_2O mixing ratios and relative differences of isotope ratios were plotted as a histogram with bin widths of 0.25 ppb (N_2O), 0.15 ‰ ($\delta^{15}N^{\alpha}$) and 0.1 ‰ ($\delta^{15}N^{\beta}$), respectively (the precision indicated is the standard deviation).

two weeks of the measuring campaign (up to 22 September), N_2O mixing ratios display tiny but typical diurnal variations with night-time increases up to 334.2 ppb, i.e., 10 ppb above background concentrations (Fig. 3). Even though these changes in N_2O mixing ratios were small in the beginning, the $\delta^{15}N^{bulk}$ values display a detectable inverse trend indicating emissions of ^{15}N depleted nitrous oxide. Substantially higher N_2O mixing ratios accompanied by $\delta^{15}N^{bulk}$ changes up to 10 ‰ were observed after the fertiliser addition on 22 September.

Long-term precision and repeatability including preconcentration and calibration was assessed analysing a pressurized air cylinder (target gas) at every fourth preconcentration run (open symbols Fig. 3). Figure 4 displays histogram plots of repeated measurements ($n = 136$) with average N_2O mixing ratios of 326.47 ± 0.36 ppb and site-specific relative isotope ratio differences of $\delta^{15}N^{\alpha} = 15.28 \pm 0.24$ ‰ and $\delta^{15}N^{\beta} = -2.91 \pm 0.17$ ‰ (the precision indicated is the standard deviation). These values are consistent with background air with minor contributions from a ^{15}N depleted N_2O emission source. The achieved long-term precision for $\delta^{15}N^{\alpha}$ and $\delta^{15}N^{\beta}$ is superior to state-of-the-art IRMS (Bernard et al., 2006; Toyoda et al., 2011a, b). Additionally, precision for N_2O mixing ratios determined by QCLAS is comparable to gas chromatography with electron capture detection (GC-ECD), the standard technique applied in global monitoring networks (Corazza et al., 2011). Besides that, as our technique has temporal averaging capabilities, the statistical uncertainty for repeated measurements (standard error of the mean) is considerably lower.

As more sensitive laser spectrometers become available, the time requirement for the adsorption step, which limits the temporal resolution of the complete analytical approach, might be significantly reduced. Another option to enhance the temporal resolving power is the less frequent determination of calibration factors for $\delta^{15}N^{\alpha}$, $\delta^{15}N^{\beta}$ and N_2O mixing ratios. This could be compensated by the preparation and use of standard gases which correspond more closely to ambient composition. Thus, timescales for N_2O preconcentration and site-specific isotopic analysis could be reduced to around 15 min.

3.2 Source appointment by N_2O isotopomer analysis

The isotopic signature of a source process can be estimated by the Keeling-plot approach where the variations in the isotopic composition are plotted against the inverse of concentration values. This technique was originally developed for carbon dioxide and its isotopologues and has been employed in numerous studies, recently also in combination with field-deployable instrumentation for continuous CO_2 isotopic analysis (McManus et al., 2010; Mohn et al., 2008; Tuzson et al., 2011). For N_2O, up to date all process studies on N_2O isotopic species had to rely on grab sampling followed by IRMS laboratory analysis because real-time analysis was not available with the required precision. Consequently, current research is based on short-term investigations with limited temporal and spatial averaging capabilities (Ostrom et al., 2010; Toyoda et al., 2011a; Yamagishi et al., 2007).

In Fig. 5, data obtained in a 24 h time interval (e.g., from 23 September noon to 24 September noon) was analysed using the Keeling plot approach. Individual data points represent the average N_2O mixing ratio and isotopic composition over 20 min of N_2O sampling during preconcentration. Assuming a two source mixing with unpolluted background air, the intercept of the linear regression line corresponds to the isotopic signature of the N_2O emitting processes for $\delta^{15}N_s^{bulk}$ and SP_s. This approach implies the assumptions that

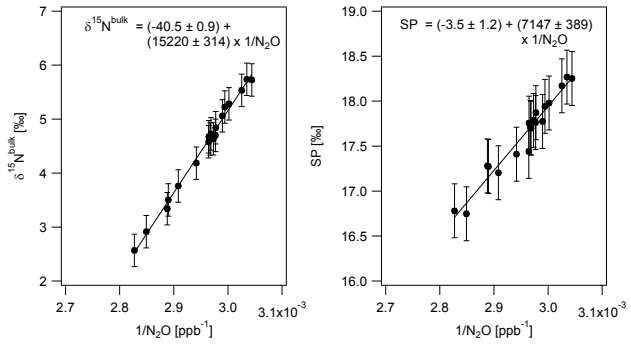

Fig. 5. Exemplary 24 h Keeling plot (23 September noon–24 September 2010 noon) after fertiliser addition. Site preference and $\delta^{15}N^{bulk}$ are plotted versus the inverse of the N_2O concentration. The intercept of the ordinary least square linear regression corresponds to the isotopic signature of the main N_2O emitting process ($\delta^{15}N_s^{bulk}$, SP_s) and is given together with its $1\,\sigma$ uncertainty.

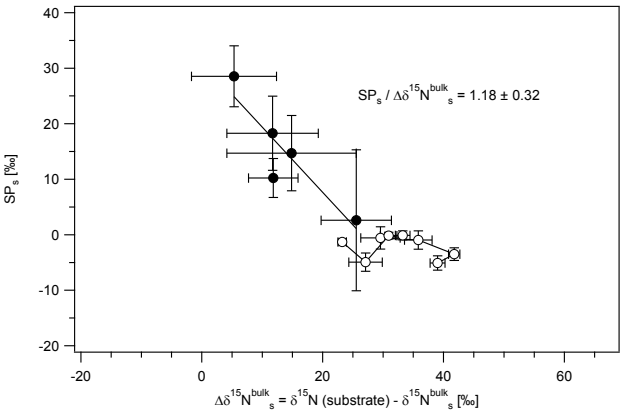

Fig. 6. SP_s versus $\Delta\delta^{15}N_s^{bulk}$ plot to interpret the biogeochemistry of soil emitted N_2O. Isotopic source signatures indicate heterotrophic or nitrifier denitrification as the main N_2O production process, with $\Delta\delta^{15}N_s^{bulk}$ values between 5 and 42 ‰. Before fertiliser application (closed symbols, 9 to 22 September, periods with N_2O concentration changes >6.5 ppb) a $SP_s/\Delta\delta^{15}N_s^{bulk}$ ratio of 1.18 ± 0.32 indicates N_2O reductase activity which ceased after fertiliser addition (open symbols, 22 to 30 September) identified by low SP_s values between 0 and -5 ‰. For $\delta^{15}N$ (substrate) 0 ‰ was assumed before fertiliser addition (before 22 September), afterwards the ^{15}N content of the applied NH_4NO_3 fertiliser (1.3 ± 0.3 ‰) was used.

the background air N_2O mixing ratio and isotopic composition and the soil microbial N_2O production pathways with their isotopic signatures are basically constant for one diurnal cycle. Although these parameters were not monitored in depth, the low scatter in the Keeling plots (i.e., Fig. 5) indicates that the model is at least adequate in demonstrating the performance of our instrumentation in capturing natural and fertiliser-induced changes in N_2O mixing ratios. The appropriateness of the above mentioned assumptions is also supported by the moderate uncertainties in the linear regression parameters (Fig. 6).

Before fertiliser addition, the diurnal variability in N_2O mixing ratios was small, in the range of 3.0 to 10.5 ppb, accompanied by only a slight shift to lower relative isotope ratio differences at higher N_2O mixing ratios. It was, nevertheless, possible to resolve these small changes and calculate daily (24 h time intervals, noon to noon) N_2O source signatures ($\delta^{15}N_s^{bulk}$, SP_s), assuming steady background N_2O mixing ratios and isotopic composition. These varied between -5 ± 7 ‰ to -26 ± 6 ‰ for $\delta^{15}N_s^{bulk}$ and 3 ± 13 ‰ to 29 ± 5 ‰ for SP_s with a temporal trend (9 to 22 September) from low to high $\delta^{15}N_s^{bulk}$ and high to low SP_s values (Fig. 6). Periods with changes in N_2O mixing ratios below 6.5 ppb (2 %) were not considered. To estimate the net isotope effect ($\Delta\delta^{15}N_s^{bulk} = \delta^{15}N\,(\text{substrate}) - \delta^{15}N_s^{bulk}$) of the microbial source process, the ^{15}N content of the substrate for N_2O production needs to be known. As the focus of the present study was on method development for ambient air monitoring and not on soil science, no supplementary soil parameters were determined. $\delta^{15}N$ of nitrate and ammonium in soils may vary considerably, depending on the nitrogen source (e.g., soil nitrogen, atmospheric deposition, fertiliser, manure) and fractionation during nitrogen transformation processes (Kendall and Doctor, 2011). In the present study for inorganic soil nitrogen a $\delta^{15}N$ content of 0 ‰ was assumed, which is in the range of data observed in a number of field studies (Durka et al., 1994; Wrage et al., 2004). This results in a net isotope effect ($\Delta\delta^{15}N_s^{bulk}$) between 5 and 26 ‰. According to pure culture studies, these values are characteristic for N_2O produced by heterotrophic denitrification or nitrifier denitrification by ammonium oxidizing bacteria (Sutka et al., 2006, 2003, 2004; Toyoda et al., 2005; Yoshida, 1988) Recent field studies confirm the importance of both processes for N_2O production in soils (Kool et al., 2011; Wrage et al., 2001). In contrast, N_2O produced by nitrifying bacteria leads to a significantly higher ^{15}N depletion with a net isotope effect ($\Delta\delta^{15}N_s^{bulk} = \delta^{15}N\,(NH_4^+) - \delta^{15}N_s^{bulk}$) between 46.9 ‰ (Sutka et al., 2006) and 68 ‰ (Yoshida, 1988).

The observed co-variation of SP_s and $\Delta\delta^{15}N_s^{bulk}$ (Fig. 6) for N_2O emitted before fertiliser application with a slope of 1.18 ± 0.32 can be attributed to a partial consumption by N_2O reductase activity of denitrifying bacteria (Koba et al., 2009; Yamagishi et al., 2007). Similar values between 1.0 and 1.2 for $SP_s/\Delta\delta^{15}N_s^{bulk}$ were reported by Ostrom et al. (2007) for N_2O reduction by two denitrifier species. The temporal trend from high to low SP_s and low to high $\Delta\delta^{15}N_s^{bulk}$ values (Fig. 6) can, thus, be interpreted as a decreasing share of N_2O reduction versus N_2O production. The N_2O versus ($N_2O + N_2$) ratio increase correlates with a night-time air temperature decrease from 13 °C to 6 °C at the nearby NABEL station (data not shown), which is consistent with the temperature dependence observed in laboratory

studies on soil samples (Avalakki et al., 1995; Bailey and Beauchamp, 1973).

After fertiliser application larger diurnal changes in N_2O mixing ratios were observed (Fig. 6). These were used to allocate 24 h isotopic source signatures, assuming stable N_2O production processes and background conditions. Furthermore, much less variation was observed in the isotopic source signatures with values between -0.1 ± 0.8 ‰ to -5.1 ± 1.3 ‰ for SP_s and 41.8 ± 0.9 ‰ to 23.2 ± 0.7 ‰ for $\Delta\delta^{15}N_s^{bulk}$. To calculate the net isotope effect ($\Delta\delta^{15}N_s^{bulk} = (\delta^{15}N$ (substrate) $- \delta^{15}N_s^{bulk})$, the ^{15}N content of the fertiliser N analysed by IRMS ($\delta^{15}N$ (NH_4NO_3) $= 1.3\pm0.3$ ‰) was applied. The resulting SP_s and $\Delta\delta^{15}N_s^{bulk}$ values are indicative for N_2O production by heterotrophic or nitrifier denitrification without or with only minor N_2O to N_2 reduction (Sutka et al., 2003, 2004, 2006; Toyoda et al., 2005; Yoshida, 1988). The observed low N_2O consumption agrees with a recent publication assuming that the $N_2O/(N_2O + N_2)$ product ratio of denitrification is positively correlated with the NO_3^- availability in soils (Senbayram et al., 2011). The successive increase in $\Delta\delta^{15}N_s^{bulk}$ suggests a shift in the isotope composition of the soil nitrate pool due to fractionation during denitrification.

4 Conclusions

This study presents to our knowledge the first real-time analysis of N_2O site-selective isotopic composition at atmospheric mixing ratios. Our approach is based on a cryogenic free instrumentation which comprises a mid-IR QCL absorption spectrometer and a fully automated N_2O preconcentration unit. During three weeks of continuous field measurements nearly 550 air samples were analysed for N_2O mixing ratios and site-specific isotopic composition. Long-term precision for $\delta^{15}N^{\alpha}$ and $\delta^{15}N^{\beta}$ was found to be superior to state-of-the-art IRMS. Additionally, precision for N_2O mixing ratios determined by QCLAS was comparable to the standard technique applied in global monitoring networks (GC-ECD).

The excellent analytical precision allowed resolving even small changes in N_2O mixing ratios and isotope composition, $\delta^{15}N^{bulk}$ and SP and calculating daily (24 h time intervals, noon to noon) source signatures ($\delta^{15}N_s^{bulk}$, SP_s) for N_2O emitted from a grassland plot. Before fertiliser application, $\Delta\delta^{15}N_s^{bulk}$ indicates heterotrophic or nitrifier denitrification as the main N_2O production pathway. Co-variation of SP_s and $\Delta\delta^{15}N_s^{bulk}$ can be attributed to a partial consumption by N_2O reductase activity of denitrifying bacteria. Denitrification remained the main N_2O production pathway after fertilization. However, the N_2O reductase activity ceased due to increased NO_3^- availability. As demonstrated in this feasibility study, continuous high precision analysis of N_2O isotopomers at atmospheric mixing ratios can be applied for identification of N_2O source processes and open a completely new field of applications.

Acknowledgements. We would like to thank Roland Bol (North Wyke Research) for ^{15}N analysis of the NH_4NO_3 fertiliser. Patrick Sturm (Empa) and Pascal Wunderlin (Eawag) are acknowledged for helpful discussions during the preparation of the manuscript. Thanks to Mario Lovric for his support during field measurements and Thomas Seitz from the Swiss National Air Pollution Monitoring Network (NABEL) for providing us supporting meteorological parameters. Heike Geilmann (MPI-BGC) is acknowledged for assistance during $\delta^{15}N^{bulk}$ analysis of primary laboratory standards. Funding from the Swiss National Foundation for Scientific Research (SNF) and the State Secretariat for Education and Research (SER) within COST-ES0806 is gratefully acknowledged. Naohiro Yoshida and Sakae Toyoda were supported by KAKENHI (17GS0203 and 23224013) of the Ministry of Education, Culture, Sports, Science and Technology and by Global Environmental Research Fund (A-0904) of the Ministry of the Environment, Japan.

Edited by: P. Werle

References

Avalakki, U. K., Strong, W. M., and Saffigna, P. G.: Measurement of gaseous emissions from denitrification of applied ^{15}N. 2. Effects of temperature and added straw, Aust. J. Soil Res., 33, 89–99, doi:10.1071/SR9950089, 1995.

Baer, D. S., Paul, J. B., Gupta, M., and O'Keefe, A.: Sensitive absorption measurements in the near-infrared region using off-axis integrated-cavity-output spectroscopy, Appl. Phys. B-Lasers O., 75, 261–265, doi:10.1007/s00340-002-0971-z, 2002.

Bailey, L. D. and Beauchamp, E. G.: Effects of temperature on NO_3^- and NO_2^- reduction, nitrogenous gas production, and redox potential in a saturated soil, Can. J. Soil Sci., 53, 213–218, doi:10.4141/cjss73-032, 1973.

Bernard, S., Röckmann, T., Kaiser, J., Barnola, J.-M., Fischer, H., Blunier, T., and Chappellaz, J.: Constraints on N_2O budget changes since pre-industrial time from new firn air and ice core isotope measurements, Atmos. Chem. Phys., 6, 493–503, doi:10.5194/acp-6-493-2006, 2006.

Brenninkmeijer, C. A. M. and Röckmann, T.: Mass spectrometry of the intramolecular nitrogen isotope distribution of environmental nitrous oxide using fragment-ion analysis, Rapid Commun. Mass Sp., 13, 2028–2033, doi:10.1002/(SICI)1097-0231(19991030)13:20<2028::AID-RCM751>3.0.CO;2-J, 1999.

Coplen, T. B.: Guidelines and recommended terms for expression of stable-isotope-ratio and gas-ratio measurement results, Rapid Commun. Mass Sp., 25, 2538–2560, 2011.

Corazza, M., Bergamaschi, P., Vermeulen, A. T., Aalto, T., Haszpra, L., Meinhardt, F., O'Doherty, S., Thompson, R., Moncrieff, J., Popa, E., Steinbacher, M., Jordan, A., Dlugokencky, E., Brühl, C., Krol, M., and Dentener, F.: Inverse modelling of European N_2O emissions: assimilating observations from different networks, Atmos. Chem. Phys., 11, 2381–2398, doi:10.5194/acp-11-2381-2011, 2011.

Crosson, E. R.: A cavity ring-down analyzer for measuring atmospheric levels of methane, carbon dioxide, and water vapor, Appl. Phys. B-Lasers O., 92, 403–408, doi:10.1007/s00340-008-3135-y, 2008.

Durka, W., Schulze, E. D., Gebauer, G., and Voerkelius, S.: Effects of forest decline on uptake and leaching of deposited nitrate determined from ^{15}N and ^{18}O measurements, Nature, 372, 765–767, doi:10.1038/372765a0, 1994.

Frame, C. H. and Casciotti, K. L.: Biogeochemical controls and isotopic signatures of nitrous oxide production by a marine ammonia-oxidizing bacterium, Biogeosciences, 7, 2695–2709, doi:10.5194/bg-7-2695-2010, 2010.

Gagliardi, G., Borri, S., Tamassia, F., Capasso, F., Gmachl, C., Sivco, D. L., Baillargeon, J. N., Hutchinson, A. L., and Cho, A. Y.: A frequency-modulated quantum-cascade laser for spectroscopy of CH_4 and N_2O isotopomers, Isot. Environ. Healt. S., 41, 313–321, doi:10.1080/10256010500384572, 2005.

Hall, B. D., Dutton, G. S., and Elkins, J. W.: The NOAA nitrous oxide standard scale for atmospheric observations, J. Geophys. Res., 112, D09305, doi:10.1029/2006JD007954, 2007.

Ishijima, K., Sugawara, S., Kawamura, K., Hashida, G., Morimoto, S., Murayama, S., Aoki, S., and Nakazawa, T.: Temporal variations of the atmospheric nitrous oxide concentration and its $\delta^{15}N$ and $\delta^{18}O$ for the latter half of the 20th century reconstructed from firn air analyses, J. Geophys. Res., 112, D03305, doi:10.1029/2006JD007208, 2007.

Janssen, C. and Tuzson, B.: A diode laser spectrometer for symmetry selective detection of ozone isotopomers, Appl. Phys. B-Lasers O., 82, 487–494, doi:10.1007/s00340-005-2044-6, 2006.

Kaiser, J., Röckmann, T., and Brenninkmeijer, C. A. M.: Complete and accurate mass spectrometric isotope analysis of tropospheric nitrous oxide, J. Geophys. Res., 108, 4476, doi:10.1029/2003JD003613, 2003.

Kendall, C. and Doctor, D. H.: Stable isotope applications in hydrological studies, in: Isotope Geochemistry, edited by: Holland, H. D. and Turekian, K. K., Elsevier Academic Press, Amsterdam, 182–226, 2011.

Koba, K., Osaka, K., Tobari, Y., Toyoda, S., Ohte, N., Katsuyama, M., Suzuki, N., Itoh, M., Yamagishi, H., Kawasaki, M., Kim, S. J., Yoshida, N., and Nakajima, T.: Biogeochemistry of nitrous oxide in groundwater in a forested ecosystem elucidated by nitrous oxide isotopomer measurements, Geochim. Cosmochim. Ac., 73, 3115–3133, doi:10.1016/j.gca.2009.03.022, 2009.

Kool, D. M., Dolfing, J., Wrage, N., and Van Groenigen, J. W.: Nitrifier denitrification as a distinct and significant source of nitrous oxide from soil, Soil Biol. Biochem., 43, 174–178, doi:10.1016/j.soilbio.2010.09.030, 2011.

McManus, J. B., Nelson, D. D., and Zahniser, M. S.: Long-term continuous sampling of $^{12}CO_2$, $^{13}CO_2$ and $^{12}C^{18}O^{16}O$ in ambient air with a quantum cascade laser spectrometer, Isot. Environ. Healt. S., 46, 49–63, doi:10.1080/10256011003661326, 2010.

Miller, B. R., Weiss, R. F., Salameh, P. K., Tanhua, T., Greally, B. R., Mühle, J., and Simmonds, P. G.: Medusa: A sample preconcentration and GC/MS detector system for in situ measurements of atmospheric trace halocarbons, hydrocarbons, and sulfur compounds, Anal. Chem., 80, 1536–1545, doi:10.1021/ac702084k, 2008.

Mohn, J., Zeeman, M. J., Werner, R. A., Eugster, W., and Emmenegger, L.: Continuous field measurements of $\delta^{13}C$-CO_2 and trace gases by FTIR spectroscopy, Isot. Environ. Healt. S., 44, 241–251, doi:10.1080/10256010802309731, 2008.

Mohn, J., Guggenheim, C., Tuzson, B., Vollmer, M. K., Toyoda, S., Yoshida, N., and Emmenegger, L.: A liquid nitrogen-free preconcentration unit for measurements of ambient N_2O isotopomers by QCLAS, Atmos. Meas. Tech., 3, 609–618, doi:10.5194/amt-3-609-2010, 2010.

Montzka, S. A., Reimann, S., Engel, A., Krüger, K., O'Doherty, S., Sturges, W. T., Blake, D., Dorf, M., Fraser, P., Froidevaux, L., Jucks, K., Kreher, K., Kurylo, M. J., Mellouki, A., Miller, J., Nielsen, O.-J., Orkin, V. L., Prinn, R. G., Rhew, R., Santee, M. L., Stohl, A., and Verdonik, D.: Ozone-depleting substances (ODSs) and related chemicals, Chapter 1, in: Scientific Assessment of Ozone Depletion: 2010, Global Ozone Research and Monitoring Project, Report No. 52, edited by: Ennis, C. A., World Meteorological Organization, Geneva, 1.1–1.108, 2011.

Nakayama, T., Fukuda, H., Kamikawa, T., Sugita, A., Kawasaki, M., Morino, I., and Inoue, G.: Measurements of the $3\nu_3$ band of $^{14}N^{15}N^{16}O$ and $^{15}N^{14}N^{16}O$ using continuous-wave cavity ring-down spectroscopy, Appl. Phys. B-Lasers O., 88, 137–140, doi:10.1007/s00340-007-2653-3, 2007.

Ostrom, N. E., Pitt, A., Sutka, R., Ostrom, P. H., Grandy, A. S., Huizinga, K. M., and Robertson, G. P.: Isotopologue effects during N_2O reduction in soils and in pure cultures of denitrifiers, J. Geophys. Res., 112, G02005, doi:10.1029/2006JG000287, 2007.

Ostrom, N. E., Sutka, R., Ostrom, P. H., Grandy, A. S., Huizinga, K. M., Gandhi, H., von Fischer, J. C., and Robertson, G. P.: Isotopologue data reveal bacterial denitrification as the primary source of N_2O during a high flux event following cultivation of a native temperate grassland, Soil Biol. Biochem., 42, 499–506, doi:10.1016/j.soilbio.2009.12.003, 2010.

Park, S., Atlas, E. L., and Boering, K. A.: Measurements of N_2O isotopologues in the stratosphere: Influence of transport on the apparent enrichment factors and the isotopologue fluxes to the troposphere, J. Geophys. Res., 109, D01305, doi:10.1029/2003JD003731, 2004.

Ravishankara, A. R., Daniel, J. S., and Portmann, R. W.: Nitrous oxide (N_2O): The dominant ozone-depleting substance emitted in the 21st century, Science, 326, 123–125, doi:10.1126/science.1176985, 2009.

Röckmann, T. and Levin, I.: High-precision determination of the changing isotopic composition of atmospheric N_2O from 1990 to 2002, J. Geophys. Res., 110, D21304, doi:10.1029/2005JD006066, 2005.

Schmidt, H. L., Werner, R. A., Yoshida, N., and Well, R.: Is the isotopic composition of nitrous oxide an indicator for its origin from nitrification or denitrification? A theoretical approach from referred data and microbiological and enzyme kinetic aspects, Rapid Commun. Mass Sp., 18, 2036–2040, doi:10.1002/rcm.1586, 2004.

Senbayram, M., Chen, R., Budai, A., Bakken, L., and Dittert, K.: N_2O emission and the $N_2O/(N_2O + N_2)$ product ratio of denitrification as controlled by available carbon substrates and nitrate concentrations, Agr. Ecosyst. Environ., 147, 4–12, doi:10.1016/j.agee.2011.06.022, 2011.

Solomon, S., Qin, D., Manning, M., Alley, R. B., Berntsen, T., Bindoff, N. L., Chen, Z., Chidthaisong, A., Gregory, J. M., Hegerl, G. C., Heimann, M., Hewitson, B., Hoskins, B. J., Joos, F., Jouzel, J., Kattsov, V., Lohmann, U., Matsuno, T., Molina, M., Nicholls, N., Overpeck, J., Raga, G., Ramaswamy, V., Ren, J., Rusticucci, M., Somerville, R., Stocker, T. F., Whetton, P., Wood, R. A., and Wratt, D.: Technical Summary, in: Climate Change 2007: The Physical Science Basis. Contribution of Working Group I

to the Fourth Assessment Report of the Intergovernmental Panel on Climate Change, edited by: Solomon, S., Qin, D., Manning, M., Chen, Z., Marquis, M., Averyt, K. B., Tignor, M., and Miller, H. L., Cambridge University Press, Cambridge, United Kingdom and New York, 91 pp., 2007.

Sutka, R. L., Ostrom, N. E., Ostrom, P. H., Gandhi, H., and Breznak, J. A.: Nitrogen isotopomer site preference of N_2O produced by Nitrosomonas europaea and Methylococcus capsulatus bath, Rapid Commun. Mass Sp., 17, 738–745, doi:10.1002/rcm.968, 2003.

Sutka, R. L., Ostrom, N. E., Ostrom, P. H., Gandhi, H., and Breznak, J. A.: Erratum: Nitrogen isotopomer site preference of N_2O produced by Nitrosomonas europaea and Methylococcus capsulatus Bath (Rapid Commun. Mass Sp., 17, 738–745, 2003), Rapid Commun. Mass Spectrom., 18, 1411–1412, doi:10.1002/rcm.1482, 2004.

Sutka, R. L., Ostrom, N. E., Ostrom, P. H., Breznak, J. A., Gandhi, H., Pitt, A. J., and Li, F.: Distinguishing nitrous oxide production from nitrification and denitrification on the basis of isotopomer abundances, Appl. Environ. Microb., 72, 638–644, doi:10.1128/AEM.72.1.638-644.2006, 2006.

Toyoda, S. and Yoshida, N.: Determination of nitrogen isotopomers of nitrous oxide on a modified isotope ratio mass spectrometer, Anal. Chem., 71, 4711–4718, doi:10.1021/ac9904563, 1999.

Toyoda, S., Yoshida, N., Miwa, T., Matsui, Y., Yamagishi, H., Tsunogai, U., Nojiri, Y., and Tsurushima, N.: Production mechanism and global budget of N_2O inferred from its isotopomers in the western North Pacific, Geophys. Res. Lett., 29, 1037, doi:10.1029/2001GL014311, 2002.

Toyoda, S., Yoshida, N., Urabe, T., Nakayama, Y., Suzuki, T., Tsuji, K., Shibuya, K., Aoki, S., Nakazawa, T., Ishidoya, S., Ishijima, K., Sugawara, S., Machida, T., Hashida, G., Morimoto, S., and Honda, H.: Temporal and latitudinal distributions of stratospheric N_2O isotopomers, J. Geophys. Res., 109, D08308, doi:10.1029/2003JD004316, 2004.

Toyoda, S., Mutobe, H., Yamagishi, H., Yoshida, N., and Tanji, Y.: Fractionation of N_2O isotopomers during production by denitrifier, Soil Biol. Biochem., 37, 1535–1545, doi:10.1016/j.soilbio.2005.01.009, 2005.

Toyoda, S., Suzuki, Y., Hattori, S., Yamada, K., Fujii, A., Yoshida, N., Kouno, R., Murayama, K., and Shiomi, H.: Isotopomer analysis of production and consumption mechanisms of N_2O and CH_4 in an advanced wastewater treatment system, Environ. Sci. Technol., 45, 917–922, doi:10.1021/es102985u, 2011a.

Toyoda, S., Yano, M., Nishimura, S., Akiyama, H., Hayakawa, A., Koba, K., Sudo, S., Yagi, K., Makabe, A., Tobari, Y., Ogawa, N. O., Ohkouchi, N., Yamada, K., and Yoshida, N.: Characterization and production and consumption processes of N_2O emitted from temperate agricultural soils determined via isotopomer ratio analysis, Glob. Biogeochem. Cy., 25, GB2008, doi:10.1029/2009GB003769, 2011b.

Tuzson, B., Henne, S., Brunner, D., Steinbacher, M., Mohn, J., Buchmann, B., and Emmenegger, L.: Continuous isotopic composition measurements of tropospheric CO_2 at Jungfraujoch (3580 m a.s.l.), Switzerland: real-time observation of regional pollution events, Atmos. Chem. Phys., 11, 1685–1696, doi:10.5194/acp-11-1685-2011, 2011.

Uehara, K., Yamamoto, K., Kikugawa, T., and Yoshida, N.: Isotope analysis of environmental substances by a new laser-spectroscopic method utilizing different pathlengths, Sensor Actuat. B-Chem., 74, 173–178, doi:10.1016/S0925-4005(00)00729-2, 2001.

Uehara, K., Yamamoto, K., Kikugawa, T., and Yoshida, N.: Site-selective nitrogen isotopic ratio measurement of nitrous oxide using 2 µm diode lasers, Spectrochim. Acta A, 59, 957–962, doi:10.1016/S1386-1425(02)00260-3, 2003.

Wächter, H. and Sigrist, M. W.: Mid-infrared laser spectroscopic determination of isotope ratios of N_2O at trace levels using wavelength modulation and balanced path length detection, Appl. Phys. B-Lasers O., 87, 539–546, doi:10.1007/s00340-007-2576-z, 2007.

Wächter, H., Mohn, J., Tuzson, B., Emmenegger, L., and Sigrist, M. W.: Determination of N_2O isotopomers with quantum cascade laser based absorption spectroscopy, Opt. Express, 16, 9239–9244, doi:10.1364/OE.16.009239, 2008.

Well, R. and Flessa, H.: Isotopologue signatures of N_2O produced by denitrification in soils, J. Geophys. Res., 114, G02020, doi:10.1029/2008JG000804, 2009.

Well, R., Flessa, H., Xing, L., Xiaotang, J., and Römheld, V.: Isotopologue ratios of N_2O emitted from microcosms with NH_4^+ fertilized arable soils under conditions favoring nitrification, Soil Biol. Biochem., 40, 2416–2426, doi:10.1016/j.soilbio.2008.06.003, 2008.

Werle, P.: Accuracy and precision of laser spectrometers for trace gas sensing in the presence of optical fringes and atmospheric turbulence, Appl. Phys. B-Lasers O., 102, 313–329, doi:10.1007/s00340-010-4165-9, 2011.

Werner, R. A., Bruch, B. A., and Brand, W. A.: ConFlo III – An interface for high precision $\delta^{13}C$ and $\delta^{15}N$ analysis with an extended dynamic range, Rapid Commun. Mass Sp., 13, 1237–1241, doi:10.1002/(sici)1097-0231(19990715)13:13<1237::aid-rcm633>3.0.co;2-c, 1999.

Wrage, N., Velthof, G. L., Van Beusichem, M. L., and Oenema, O.: Role of nitrifier denitrification in the production of nitrous oxide, Soil Biol. Biochem., 33, 1723–1732, doi:10.1016/s0038-0717(01)00096-7, 2001.

Wrage, N., Lauf, J., del Prado, A., Pinto, M., Pietrzak, S., Yamulki, S., Oenema, O., and Gebauer, G.: Distinguishing sources of N_2O in European grasslands by stable isotope analysis, Rapid Commun. Mass Sp.., 18, 1201–1207, doi:10.1016/j.soilbio.2003.09.009, 2004.

Yamagishi, H., Westley, M. B., Popp, B. N., Toyoda, S., Yoshida, N., Watanabe, S., Koba, K., and Yamanaka, Y.: Role of nitrification and denitrification on the nitrous oxide cycle in the eastern tropical North Pacific and Gulf of California, J. Geophys. Res., 112, G02015, doi:10.1029/2006JG000227, 2007.

Yoshida, N.: ^{15}N-depleted N_2O as a product of nitrification, Nature, 335, 528–529, doi:10.1038/335528a0, 1988.

Yoshida, N. and Toyoda, S.: Constraining the atmospheric N_2O budget from intramolecular site preference in N_2O isotopomers, Nature, 405, 330–334, doi:10.1038/35012558, 2000.